Chapter 2

KINETICS AND MECHANISMS FOR TCE OXIDATION BY PERMANGANATE

Y. E. Yan and F. W. Schwartz

Introduction

There is considerable interest in the in-situ oxidative degradation of chlorinated ethenes with a metal-oxo reagent (1-5). In terms of remediating contaminated ground water, this method is attractive due to the rapid degradation of chlorinated ethenes, the non-reactive nature of the reagent with carbonate and bicarbonate, the ease of field implementation, and the relatively low costs (1,5,6). Degradation kinetics for five chlorinated ethenes, including PCE, TCE, and three isomers of DCE were reported by (7). TCE degradation was postulated to involve the following three sequential reactions:

$$C_2HCl_3 + MnO_4^- \xrightarrow{k_1} I \xrightarrow{k_2} \gamma CA + MnO_2 + 3Cl^- \quad (2.1)$$

$$\gamma CA \xrightarrow{k_3\ (MnO_4^-)} \eta\, CO_2 \quad (2.2)$$

where I is a cyclic complex, CA are various carboxylic acids, γ and $\eta$are stoichiometric coefficients, and k_1, k_2, and k_3 are rate constants. In the first reaction, TCE disappearance was found to be independent of pH. Complete chlorine liberation thought to occur in the second step of Eq. 2.1. However, the second and third reactions have not been studied in detail. Other work indicates that the oxidation of alkene and its products is highly pH dependent and that both permanganate and hydroxyl ions compete for a common cyclic intermediate (8). The purpose of our study here was to describe the kinetics and mechanisms involved with TCE oxidation by permanganate. Specific objectives of the study are (i) to identify reaction products, (ii) to elucidate reaction pathways and their pH dependence, (iii) to develop a kinetic model, and (iv) to determine the rate constants for all major reactions in $KMnO_4$-TCE-H_2O system.

Experimental Methods

Materials

Radiolabeled [1,2-^{14}C] TCE (3.1 mCi/mmol) was purchased from Sigma Chemical Co. (St. Louis, MO) and diluted with methanol in a 10-ml glass volumetric flask and stored at 4°C in the dark. Carboxylic acids were obtained from Fluke (Buchs, Switzerland) with purity 99+% and used as received. All other chemicals were of the highest purity available and were described previously (7).

Product Studies and Kinetic Experiments

With TCE oxidation reaction by permanganate, carboxylic acids and carbon dioxide would be expected as the major intermediate and final products (7). Two types of kinetic experiments were designed to identify the carboxylic acids and to trace CO_2 formation. Each type consists of three experiments conducted at pHs 4, 6, and 8 and each experiment has one set of vials with two or three replicates and one control vial containing only TCE aqueous solution.

For investigating carboxylic acid distributions over time, a first kinetic experiment was conducted in 50-ml glass vials with PTFE/silicone septum-lined screw-top caps. Each vial was filled with a 50-ml TCE solution of 0.1 mM. The experiment began by injecting 5-ml of $KMnO_4$ of 6.3 mM through the septum. A second needle enabled an equal volume of TCE solution to be displaced. Vials were placed on a vibratory shaker until sampled. At each sampling time, one vial was taken. A 1-ml aliquot of reaction solution from the vial was transferred to a volumetric flask with appropriate dilution following immediate TCE analysis. To quench the reaction, 1-ml thiosulfate from the stock solution was added to the vial. The quenched solution was centrifuged at 3000 rpm for 20 minutes and filtered by 0.2-µm filter to separate the precipitated manganese dioxide. After filtration, the solutions were withdrawn for carboxylic acid analysis.

To trace the CO_2 production, we undertook a second kinetic experiment with radiolabeled ^{14}C TCE. To maintain the same initial conditions as the first kinetic test, experiments began with the addition of 0.1-ml permanganate stock solution to a set of 3-ml test tubes filled with a 2.9-ml of a 0.093 mM TCE solution. At predetermined intervals, a test tube was sacrificed with the reaction quenched by adding 0.1-ml of thiosulfate from the stock solution. The test solution was then analyzed for CO_2.

Chemical Analysis

The organic acids were analyzed on a Waters high performance liquid chromatography (HPLC) fitted with a Bio-Rad Aminex HPX-87H column (300 × 7.8 mm I.D.). CO_2 was determined by retaining CO_2 under basic conditions and stripping CO_2 under acidic conditions. This method was adapted from (9). TCE concentrations were determined as described in (7).

Results and Discussion

Products

In the experiments for identifying products, a 0.09 mM TCE solution was reacted with 0.63 mM permanganate. The solution was phosphate-buffered and had an ionic strength of

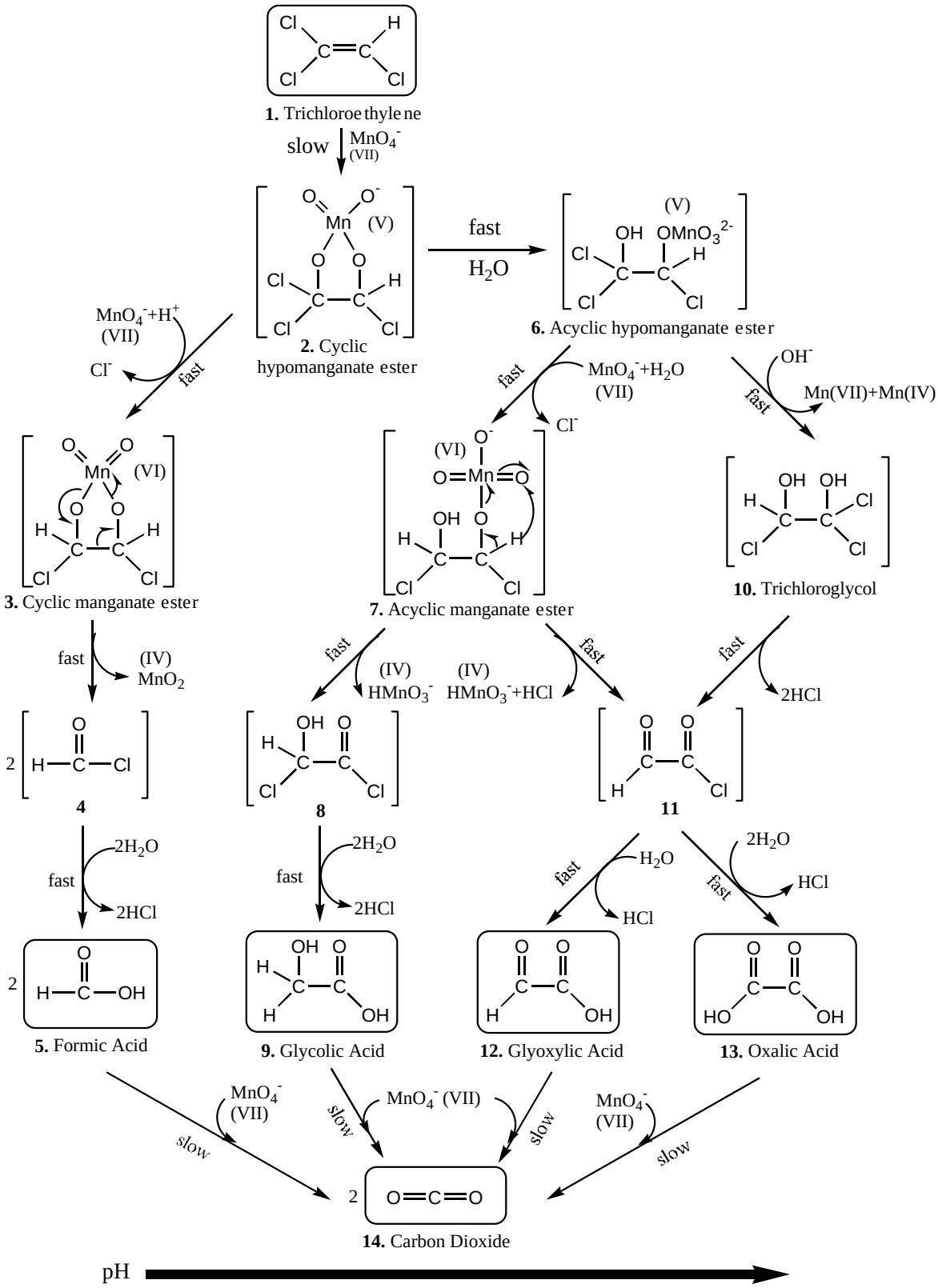

Figure 2.1. Proposed TCE oxidation pathways. Shadowed boxes are products identified in this study.

0.05 M at pH 4, 6, and 8, respectively. Four carboxylic acids, formic, oxalic, glyoxylic, and glycolic acids, were identified in the system as intermediate products. Either formic or oxalic acid predominated, depending on the pH. One hour after the reaction started, a maximum of 43% of the initial TCE was converted to either formic or oxalic acid and up to 25% of the TCE was transformed to glyoxylic acid. Glycolic acid was produced in small quantities (<2%).

The radiolabled product analysis indicates that the majority of TCE was eventually transformed to CO_2, the final product. Assuming TCE is stoichiometrically converted to CO_2, 57-88% of the initial TCE, varying depending on pH, was converted to CO_2 when the experiments were terminated at 8 hours.

The proposed chemical pathways for TCE oxidation (Figure 2.1) were developed from a basic understanding of alkene oxidation by permanganate in organic synthesis chemistry (8,10,11). The products and intermediates in the shadowed boxes were identified in our experiments. TCE oxidation is initiated by the attack of permanganate ion, as an electrophile, on the carbon-carbon double bond (7). An organometallic compound, cyclic hypomanganate ester **2** is formed via an activation complex in transition state (10,12-13). The rapid decomposition of cyclic ester **2** can follow several different pathways in an aqueous system such as oxidative hydrolysis and hydrolysis.

Oxidative hydrolysis transforms cyclic hypomanganate ester **2** rapidly to cyclic manganate (VI) ester **3** to form formic acid **5** via **4**. Two other possible pathways involve the hydrolysis of cyclic ester **2** to acyclic hypomanganate (V) ester **6**. The acyclic manganate (VI) ester **7**, oxidatively hydrolyzed from **6**, may undergo rapid electron transfer and then either hydrolysis to form glycolic acid **9** via **8** or release of one hydrogen chloride and hydrolysis to form glyoxylic acid **12** or oxalic acid **13** via **11**. In weak alkalinic to alkalinic solutions, acyclic ester **6** may simply hydrolyze to trichloroglycol **10**, which rapidly releases two hydrogen chlorides. This compound is subsequently hydrolyzed to either glyoxylic acid **12** or oxalic acid **13**. Carboxylic acids are further oxidized to carbon dioxide at a relatively slow rate.

The liberation of chlorine substitutes is hypothesized as a series of reactions, involving the transformation of hypomanganate ester to manganate ester, the electron transfer to release hydrogen chloride, and hydrolysis. A stoichiometrically consistent release of chloride was observed along with disappearance of TCE (7). Thus, the decomposition of the ester with chloride release is a very rapid process, which is much faster than its formation.

Kinetic Equations for TCE Oxidation

TCE oxidation by permanganate ion generally involves the formation and decomposition of cyclic hypomanganate ester (CHME), and the oxidation of carboxylic acids, based on the TCE transformation pathways in Figure 2.1. A second order reaction for the formation of CHME was suggested by (5):

$$C_2HCl_3 + MnO_4^- \xrightarrow{k_{1p}} CHME \qquad (2.3)$$

where k_{1p} is a second-order rate constant. The decomposition of CHME via various pathways to form major carboxylic acids and the release of chlorides can be described by Eqs. 2.4-6:

$$\alpha CHME + \beta H_2O \xrightarrow{k_{2a}} 2\alpha HCOOH + \alpha MnO_2 + 3\alpha Cl^- + \gamma H^+ \qquad (2.4)$$

$$\alpha CHME + \eta H_2O \xrightarrow{k_{2b}} \alpha OHC-COOH + \alpha MnO_2 + 3\alpha Cl^- + \upsilon H^+ \qquad (2.5)$$

$$\alpha CHME + \xi H_2O \xrightarrow{k_{2c}} \alpha HOOC-COOH + \alpha MnO_2 + 3\alpha Cl^- + \zeta H^+ \qquad (2.6)$$

where α, β, γ, η, ν, ξ and ζ are stoichiometric coefficients and k_{2a}, k_{2b}, and k_{2c} are rate constants for the formation of formic, glyoxylic, and oxalic acids, respectively.

The oxidation of formic, glyoxylic, and oxalic acids by permanganate involves a series of reactions. Most studies, however, have shown that the reaction at a rate limiting step can be described by second-order reaction for formic and oxalic acids (14-16). By analogy with the oxidation of formic and oxalic acids, it is reasonable to assume a second-order reaction for glyoxylic acid due to its similar structure to the other two acids. The rate laws for these three oxidation reactions are shown in Eqs. 2.7-9 (Table 2.1). With an excess of MnO_4^- in aqueous media at a fixed pH, the order of kinetic reaction can be reduced. The rates of disappearance/appearance for TCE, major intermediates and final product are summarized in Table 2.1, Eqs. 2.10-15.

Estimation of Rate Constants

To find the rate constants for transformation and/or formation of TCE, three carboxylic acids, and CO_2, equations of 10-15 were solved analytically using Laplace transformation. The solutions for TCE, formic, glyoxylic, and oxalic acids in terms of normalized concentration are:

$$\frac{[TCE]}{[TCE]_0} = e^{-k_1 t} \qquad (2.16)$$

$$\frac{[C_t]_l}{[TCE]_0} = m k_1 k_{2l} \sum_i \frac{e^{-k_i t}}{\prod_{j(j\neq i)} (k_j - k_i)} \quad \begin{matrix} i,j=1,2,\text{and}3l; \\ l=a,b,\text{and}c; \end{matrix} \quad m = \begin{cases} 2 & l=a \\ 1 & l=b,c \end{cases}; \qquad (2.17)$$

where $[C_t]_l$ is the concentration of the carboxylic acids and the subscript l =a, b, and c denotes formic, glyoxylic, and oxalic acids, respectively. The formation of CO_2 can be described as

$$\frac{[CO_2]}{[TCE]_0} = 2\left\{1 - k_1 \sum_{l=a}^{c} \left(k_{2l} k_{3l} \sum_i \frac{e^{-k_i t}}{k_i \prod_{j(j\neq i)} (k_j - k_i)} \right)\right\} \quad i, j=1,2,\text{and}3l \qquad (2.18)$$

To establish a kinetic model, the seven rate constants, k_1,

Table 2.1: Listing of kinetic equations.

Equation	No
$\frac{d[HCOOH]_t}{dt}=-k_{3ap}[HCOOH]_t[MnO_4^-]$	2.7
$\frac{d[OHC-COOH]_t}{dt}=-k_{3bp}[OHC-COOH]_t[MnO_4^-]$	2.8
$\frac{d[HOOC-COOH]_t}{dt}=-k_{3cp}[HOOC-COOH]_t[MnO_4^-]$	2.9
$\frac{d[C_2HCl_3]}{dt}=-k_1[C_2HCl_3] \qquad k_1=k_{1p}[MnO_4^-]$	2.10
$\frac{d[CHME]}{dt}=k_1[C_2HCl_3]-k_2[CHME] \qquad k_2=k_{2a}+k_{2b}+k_{2c}$	2.11
$\frac{d[HCOOH]_t}{dt}=2k_{2a}[CHME]-k_{3a}[HCOOH]_t \quad k_{3a}=k_{3ap}[MnO_4^-]$	2.12
$\frac{d[HCO-COOH]_t}{dt}=k_{2b}[CHME]-k_{3b}[OHC-COOH]_t \; k_{3b}=k_{3bp}[MnO_4^-]$	2.13
$\frac{d[HOOC-COOH]_t}{dt}=k_{2c}[CHME]-k_{3c}[HOOC-COOH]_t \, k_{3c}=k_{3cp}[MnO_4^-]$	2.14
$\frac{d[CO_2]}{dt}=k_{3a}[COOH]_t+2k_{3b}[OHC-COOH]_t+2k_{3c}[HOOC-COOH]_t$	2.15
$\frac{d[HCOOH]_t}{dt}=-(k_{3ap1}[HCOOH]+k_{3ap2}[HCOO^-])[MnO_4^-] =-\left(\frac{k_{3ap1}[H^+]+k_{3ap2}K_a}{[H^+]+K_a}\right)[HCOOH]_t[MnO_4^-]$	2.25
$\frac{d[HOC-COOH]_t}{dt}=-(k_{3bp1}[HOC-COOH]+k_{3bp2}[HOC-COO^-])[MnO_4^-] =-\left(\frac{k_{3bp1}[H^+]+k_{3bp2}K_a}{[H^+]+K_b}\right)[HOC-COOH]_t[MnO_4^-]$	2.26
$\frac{d[HOOC-COOH]_t}{dt}=-(k_{3cp1}[HOOC-COOH]+k_{3cp2}[HOOC-COO^-] +k_{3cp3}[^-OOC-COO^-])[MnO_4^-] =-\left(\frac{k_{3cp1}[H^+]^2+k_{3cp2}K_{c1}[H^+]+k_{3cp3}K_{c1}K_{c2}}{K_{c1}K_{c2}+K_{c1}[H^+]+[H^+]^2}\right)[HOOC-COOH]_t[MnO_4^-]$	2.27

subscript t for each acid denotes the total concentration; k_1, k_{3a}, k_{3b}, and k_{3c} are pseudo-first-order rate constants; k_{2a}, k_{2b}, and k_{2c} are first-order rate constants; k_{3ap}, k_{3bp}, and k_{3cp} are second-order rate constants; k_{3ap1}, k_{3ap2}, k_{3bp1}, k_{3bp2}, k_{3cp1}, k_{3cp2}, and k_{3cp3} are rate constants.

k_{2a}, k_{2b}, k_{2c}, k_{3a}, k_{3b}, and k_{3c} need to be estimated using kinetic data from the TCE oxidation experiments. Accordingly, the kinetic experiments, described previously, were conducted with H_3PO_4-K_2HPO_4- KH_2PO_4-NaOH buffer at pHs 4, 6, and 8. The concentrations of TCE, the intermediates (including formic, glyoxylic and oxalic acids), and the final product, CO_2 were measured with time. Mass balances in these experiments ranged from 0.84 to 1.09. The results indicate that the experiments were well controlled, even though various analytical procedures were involved.

Rate constants were estimated with Eqs. 2.16-17 by fitting the measured concentration data. The fitted results (Figure 2.2) agree well with the experimental data across a pH range of 4 to 8. With the pseudo-first-order rate constant k_1 ranging from 4.11 $\times$ 10^{-4} to 4.30 $\times$ 10^{-4} s^{-1} (Table 2.2), the second-order rate constant k_{1p}, defined in Eq. 2.10, can be calculated. The calculated k_{1p} in the range of 0.65 - 0.68 M^{-1} s^{-1} agrees with (7) (i.e., k=0.67±0.03 M^{-1} s^{-1}).

To choose an appropriate k_2 for the second step in TCE oxidation, the concentration data for the carboxylic acids were fitted with Eq. 2.17 using various ratios of k_2 to k_1. The results indicate that determination coefficient (r^2) for curve fittings was improved with increasing k_2/k_1 ratio and reaches 0.9 at k_2/k_1>10. The large k_2/k_1 ratio supports the idea that the decomposition of

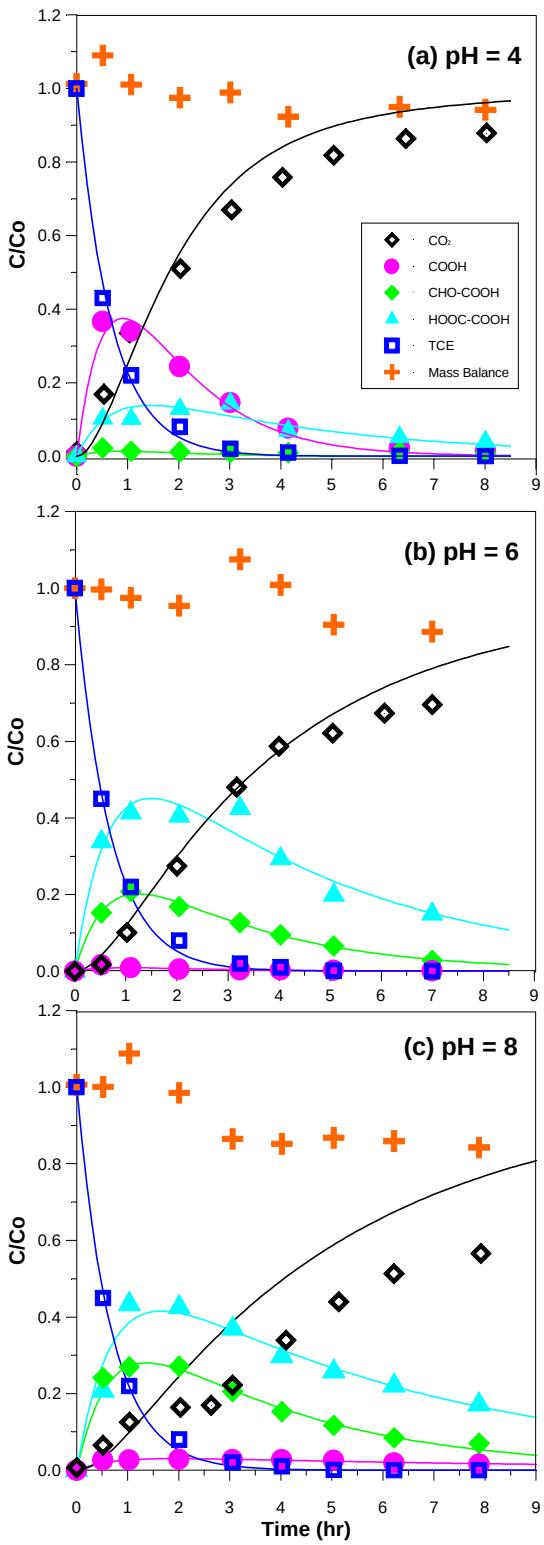

Figure 2.2. Product distribution with time in TCE oxidation at pH 4 (a), pH 6 (b) and pH 8 (c). Lines for TCE and carboxylic acids represent best fits using eqs 16-17, whereas the line for CO_2 is calculated by eq 18 using rate constants from the previous curve fitting.

cyclic ester is much faster than its formation, as suggested by (7,8). When $k_2 > 10^2\ k_1$, r^2 does not show any obvious improvement. All other rate constants (k_{2a}, k_{2b}, k_{2c}, k_{3a}, k_{3b}, and k_{3c}) remain constant with increasing k_2/k_1. Thus, $k_2 = 10^2\ k_1$ was assumed in all curve fittings. The ratios, k_{2a}/k_2, k_{2b}/k_2, and k_{2c}/k_2, represent the fraction of the total decomposition rate along each pathway and quantify the contribution from the various pathways in Figure 2.1. Their values (Table 2.2) suggest that the pathway leading to formic or oxalic acid is dominant in the decomposition process.

The pseudo-first-order rate constants, k_{3a}, k_{3b}, and k_{3c}, describe the oxidation of formic, glyoxylic, and oxalic acids in the final step. Compared to the other steps in TCE oxidation, the oxidation rates for the carboxylic acids are slower than any of the rates in the previous steps. The second-order rate constants, k_{3ap}, k_{3bp}, and k_{3cp}, can be calculated with Eqs. 2.12-14. k_{3ap} for the oxidation of formic acid ranges from 0.075 to 0.16 $M^{-1}s^{-1}$. These results compare well with the range of 0.003-0.25 $M^{-1}s^{-1}$ obtained by (17). The observed range in k_{3c} values, 0.073-0.11 $M^{-1}s^{-1}$, for oxalic acid is also consistent with k = 0.005-0.02 $M^{-1}s^{-1}$ (16). Based on the estimated rate constants, the oxidation rates for formic and glyoxylic acids are greater than oxalic acid over a pH range of 4-8.

Using all the estimated rate constants, the calculated accumulation of CO_2 is plotted in Figure 2.2. The results for CO_2 are in general agreement with the experimental data, except at pH 8 where the predicted CO_2 is higher than the observed at later time. This overestimation may result from the adsorption of carboxylic acids on MnO_2, which is more readily precipitated at pH 8 than other pH conditions. Because the precipitates were left in the filtrates in our experiments for acid analysis, acid adsorption on MnO_2 could cause a mass deficiency, which occurs at late time (Figure 2.2c). Consequently, the rate constant k_3 at pH 8 may be slightly overestimated.

Effects of pH and Temperature

During the first step in TCE oxidation, the rate constant k_1 does not show strong correlation with pH. Our previous study (7) indicated that (i) the variation of k_1 at different pH is small and within the experimental error and (ii) the second-order rate constant k_{1p} is equal to 0.67±0.03 $M^{-1}\ s^{-1}$. Thus, the rate of TCE disappearance is independent of pH. However, the fate of hypomanganate ester and the product distribution are strongly dependent on pH. At pH = 4, the transformation of cyclic ester to formic acid is overwhelmingly dominant (k_{2a}/k_2 = 0.77). At pH of 6-8, decomposition favors the formation of oxalic and glyoxylic acids ($(k_{2b}+ k_{2c})/k_2$ = 0.95-96). Most of cyclic ester reacts to form oxalic and glyoxylic acids in this higher pH range.

The rate constants (k_{3a}, k_{3b}, and k_{3c}) for oxidation of carboxylic acids are strongly correlated with pH over a range of 4-8 (Figure 2.3). With decreasing pH, the oxidation rates (k_3) increase for all three carboxylic acids. This pH effect on k_3 results in the relatively rapid formation of CO_2 at low pHs, as

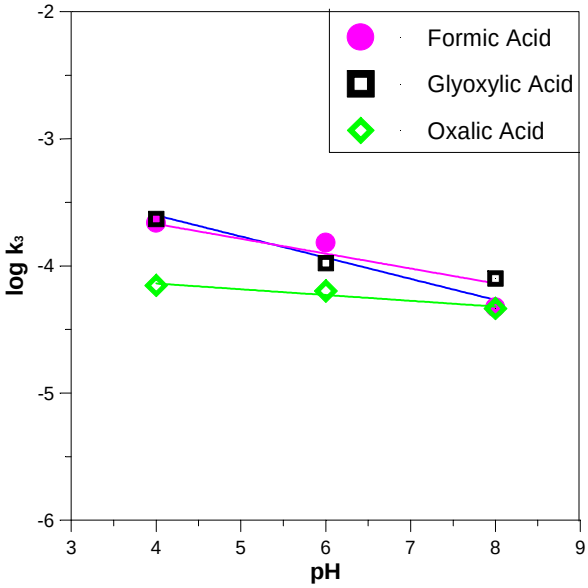

Figure 2.3. Dependence of the pseudo-first-order rate constants (k_{3a}, k_{3b}, and k_{3c}) on pH for oxidation of carboxylic acids. The reaction involved reacting 0.09 mM TCE with 0.63 mM MnO_4^- in a phosphate buffered aqueous solution at ionic strength 0.05 M.

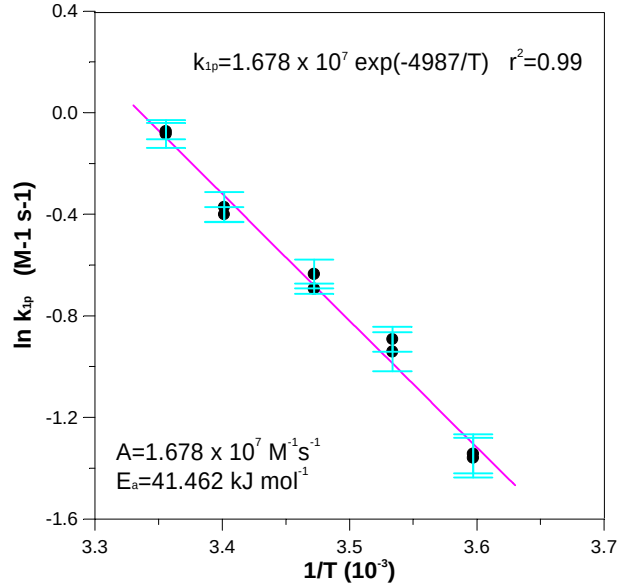

Figure 2.4. Arrhenius plot for the oxidation of TCE (0.06 mM) by potassium permanganate (1 mM) in a phosphate buffered solution at ionic strength 0.05M and pH 7.1. Error bars are standard deviation for each estimated second-order rate constant k_1.

compared to higher pHs.

In order to investigate the effect of temperature on the rate TCE transformation, five sets of duplicated kinetic experiments were performed at temperatures varying from 5 to 25 ^oC. All experiments were initiated by reacting 0.06 mM TCE with excess of MnO_4^- (1mM) at pH 7 and an ionic strength of 0.05 M. The estimated logarithm of the second-order rate constant k_{1p} from the experiments is plotted against the reciprocal of temperature in Figure 2.4. The dependence of k_{1p} on temperature, as expected, follows the Arrhenius equation. The activation energy (E_a) and preexponential (A) were calculated and are listed in Figure 2.4. These values can provide a rate constant, k_{1p}, at any temperature relevant to ground water.

Based on the E_a=41.46 kJ/mol and A=1.678×10^7 M^{-1} s^{-1}, activation parameters, $\Delta H^‡$ and $\Delta S^‡$, can be calculated. The low activation enthalpy ($\Delta H^‡$ = 39 kJ/mol) obtained here is comparable to the results from many other studies in alkene oxidation by permanganate. This result indicates that initial step of TCE oxidation may proceed via a similar transition state as other alkene oxidation. The negative entropy ($\Delta S^‡$ = -14 J/mol) is consistent with a bimolecular reaction in which the transient intermediate may be highly structured and possibly solvated.

Proposed Mechanism for TCE Oxidation

The fact that the loss of TCE is independent of pH but that the nature and distribution of products are highly dependent on pH strongly supports the existence of a short-lived intermediate in the initial stage of oxidation. In the classical view, as summarized by (10), the formation of cyclic ester involves a 3+2 electrocyclic addition of permanganate ion to the carbon-carbon double bond

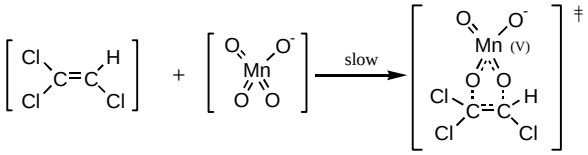

(2.19)

where the superscript ‡ indicates that the intermediate is activated at transition state. The modern ideas on alkene

Table 2.2. Rate constants obtained for TCE transformation pathways using equations, 16-17. Estimation was based on experiments conducted with an initial concentration of 0.63 mM MnO_4^-. $k_2 > 10^2$ k_1.

pH	k_1 10^{-4} s^{-1}	k_{2a}/k_2	k_{3a} 10^{-4} s^{-1}	r^2	k_{2b}/k_2	k_{3b} 10^{-4} s^{-1}	r^2	k_{2c}/k_2	k_{3c} 10^{-4} s^{-1}	r^2
4	4.30	0.77	2.19	0.98	0.03	2.34	0.98	0.20	0.70	0.95
6	4.11	0.02	1.53	0.91	0.32	1.05	0.99	0.63	0.64	0.95
8	4.11	0.04	0.47	0.97	0.42	0.80	0.99	0.55	0.46	0.95

oxidation by permanganate have been advanced by (12, 18). The initial formation of transient organometallic intermediate proceeds with 2+2 insertion of an alkene π bond directly into a metal-oxo bond of manganese.

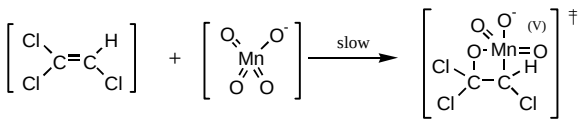

(2.20)

This reaction mechanism more reasonably explains why permanganate ion with electron-rich oxygen termini could attack carbon-carbon double bond electrophilically. The attack is controlled by orbital-overlap via delocalized charge-transfer interaction rather than net-charge (13, 19). In the initial TCE oxidation, TCE with electron-withdrawing group (Cl) is more likely attacked by permanganate ion via a transition state in Eq. 2.20. This reaction mechanism may also favor trans isomers with a charge-transfer interaction in the transition state (19). This view is supported by our early result that trans-DCE showed much greater reactivity than cis-DCE (7).

The small enthalpy $\Delta H^{\ddagger}$ (39 kJ/mol) and negative entropy $\Delta S^{\ddagger}$ (-14 J/mol) are consistent with the observations of the oxidation of other alkenic substrates by permanganate under various conditions, even though their products are different. The results suggest that TCE oxidation proceeds via similar transition states but that these transformation products are subjected to various post-transition-state reactions, which are highly dependent on reaction conditions.

The existence of various reaction pathways is evidenced by the formation of different intermediate products as a function of pH. At pH 4, the decomposition of cyclic ester **2** involves both oxidative hydrolysis (following carbon bond cleavage) to form formic acid and hydrolysis (with subsequent reactions) to form oxalic acid (Figure 2.1). The calculated ratios of rate constants (k_{2a}/k_2 and k_{2c}/k_2) indicate that the former reaction pathway is predominant (77% of total production), while the latter one is much less importance (20%). With increasing pH, almost all the cyclic esters are hydrolyzed via **6**. Products are further decomposed via oxidative hydrolysis, hydrolysis and electron transfer to form either glyoxylic or oxalic acid. Decomposition of acyclic ester **7** via **8** to form glycolic acid is insignificant. The estimated k_2/k_1 ratio from our kinetic data also supports the postulate that the decomposition of cyclic ester is much faster than its formation. The series of reactions, during the fast ester decomposition, liberate almost all the chlorine substitutes on TCE (7).

In the final step, the oxidation of carboxylic acids is relatively slow compared to the previous steps. The oxidation may involve hydride abstraction by permanganate ion (20) and carbon-carbon bond cleavage. In the aqueous solution, carboxylic acids can be dissociated:

$$HCOOH \Leftrightarrow HCOO^- + H^+ \quad pK_a = 3.74 \qquad (2.21)$$

$$HOC-COOH \Leftrightarrow HOC-COO^- + H^+ \quad pK_b = 3.34 \qquad (2.22)$$

$$HOOC-COOH \Leftrightarrow HOOC-COO^- + H^+ \quad pK_{c1} = 1.27 \qquad (2.23)$$

$$HOOC-COO^- \Leftrightarrow {}^-OOC-COO^- + H^+ \quad pK_{c2} = 4.28 \qquad (2.24)$$

where K_a, K_b, K_{c1}, and K_{c2}, are ionization constant for formic, glyoxylic and oxalic acids, respectively. If all species are considered to react independently with permanganate, Eqs. 2.7-9 can be further developed to Eqs. 2.25-27 (Table 2.1). Because the pH range of 4-8 is higher than pK_a pK_b, pK_{c1}, $[H^+] << K_a$, $[H^+] << K_b$ and $[H^+]^2 << K_{c1}K_{c2}$ and $K_{c1}[H]^+$. As compared to Eqs. 2.25-27 with 2.7-9, the second-order rate constants for oxidation of formic, glyoxylic, and oxalic acids are

$$k_{3ap} = \frac{k_{3ap1}}{K_a}[H^+] + k_{3ap2} \qquad (2.28)$$

$$k_{3bp} = \frac{k_{3bp1}}{K_b}[H^+] + k_{3bp2} \qquad (2.29)$$

$$k_{3cp} = \frac{k_{3cp1}[H^+]^2 + k_{3cp2}K[H^+] + k_{3cp3}K_{c1}K_{c2}}{K_{c1}K_{c2} + K_{c1}[H^+]} \qquad (2.30)$$

The relationship between logarithm of second-order rate constants with pH shown in Figure 2.3 is consistent with the mechanism described by Eqs. 2.28-30. Because of the relatively high oxidation rate of carboxylic acids at low pH, as illustrated in Figures 2.2, CO_2 is accumulated more rapidly with decreasing pH.

Acknowledgements

We thank Drs. O. H. Tuovinen, Y. P. Chin , S. Traina for their advice and assistance. This material is based upon work supported by the U. S. Department of Energy under Grant No. DE-FG07-96ER14735.

References

(1) Vella, P. A.; Veronda, B., In *Chemical Oxidation Technologies for the Nineties*, Eckenfelder, W. W., ed., Technomic Publishing, Lancaster, Basel, **1992**.

(2) Truax, C.M. A. Sc. *Thesis*, Univ. Waterloo, Waterloo, Ontario, Canada, **1993**.

(3) Yan Y. E.; Schwartz F. W. *EOS*, **1995**, 76(46), F247.

(4) Gates D. D.; Siegrist, R. L.; Cline, S. R. In *Proceedings of 88th Annual Meeting and Exhibition*, Air & Waste Management Assoc., San Antonio, Texas, June 18-23, **1995**.

(5) Schnarr, M.; Truax, C.; Farquhar, G.; Hood E.; Gonullu, T.; Stickney, B. *J. Contam. Hydrol*. **1998**, 29, 205-224.

(6) Vella, P. A. In *Proceedings of 3rd Intl. Conf. on Advanced Oxidation Technologies for Water and Air Remediation*, Cincinnati, Ohio, Oct. 26-29, **1996**, 119-120.

(7) Yan, Y. E. and Schwartz, F. W. *J. Contam. Hydrol.* **1999**, 37, 343-365.

(8) Wiberg, K. B.; Saegebarth, K. A. *J. Am. Chem. Soc.* **1957**, 79, 2822-2824.

(9) Kriegman-King, M. R.; Reinhard, M. *Environ. Sci. Technol.* **1992**, 26, 2198-2206.

(10) Freeman, F. *Reviews on Reactive Species in Chemical Reactions* **1976**, 1, 179-226.

(11) Lee, D. G.; Chen, T. *J. Am. Chem. Soc.* **1989**, 111, 7534-7538.

(12) Sharpless, K. B.; Teranishi, A. Y.; Backvall, J. E. *J. Am. Chem. Soc.* **1977**, 99, 3120-3128.

(13) Lee, D. G.; Brown, K. C. *J. Am. Chem. Soc.* **1982**, 104, 5076-5081.

(14) Berka, A.; Koreckova, J. *Analytical Letters* **1973**, 6, 1113-1123.

(15) Rodriguez, J.; Sanchez Burgos, F. *Ion (Madrid)* **1975**, 35, 241-245.

(16) Mahmood, A. J.; Begum, M. *Dacca University Studies, Pt. B.*, **1975**, 23, 51-64.

(17) Pérez-Benito, J. F.; Arias, C.; Brillas, E. *Int. J. Chem. Kinet.* **1990**, 22, 261-287.

(18) Rappe, A. K. and Goddard, W. A. III. *J. Am. Chem. Soc.* **1982**, 104, 448-456.

(19) Toyoshima, K.; Okuyama, T.; Fueno, T. *J. Organic Chem.* **1980**, 45, 1600-1604.

(20) Gardner, K. A.; Mayer, J. M. *Science* **1995**, 269, 1849-1851.

HOME BACK NEXT